J Physiol 590.15 (2012) pp 3421–3430

The Journal of Physiology

The *Arabidopsis* central vacuole as an expression system for intracellular transporters: functional characterization of the Cl^-/H^+ exchanger CLC-7

Alex Costa[1], Paul Vijay Kanth Gutla[2], Anna Boccaccio[2], Joachim Scholz-Starke[2], Margherita Festa[3], Barbara Basso[3], Ilaria Zanardi[2], Michael Pusch[2], Fiorella Lo Schiavo[1], Franco Gambale[2] and Armando Carpaneto[2]

[1] *University of Padova, Via U. Bassi 58/B, 35131 Padova, Italy*
[2] *Institute of Biophysics – CNR, Via De Marini 6, 16149 Genova, Italy*
[3] *Institute of Biophysics – CNR, U.O.S. di Milano, Via Giovanni Celoria 26, 20133 Milano, Italy*

Key points

- Ion transport proteins in intracellular membranes of eukaryotic cells play key roles in many physiological and pathological processes.
- The function of many of these transporters is poorly understood, because their intracellular localization makes them difficult to study.
- Here, we used the large organelle of plant cells, the central vacuole, as a novel system to study an intracellular transporter from animal cells.
- Our data showed that the lysosomal chloride transporter CLC-7 from rat constitutes a functional transport protein in the central vacuole of the model plant *Arabidopsis thaliana* (thale cress).
- This novel approach has the potential to elucidate the transport properties of further, poorly studied intracellular ion channels and transporters.

Abstract Functional characterization of intracellular transporters is hampered by the inaccessibility of animal endomembranes to standard electrophysiological techniques. Here, we used *Arabidopsis* mesophyll protoplasts as a novel heterologous expression system for the lysosomal chloride–proton exchanger CLC-7 from rat. Following transient expression of a rCLC-7:EGFP construct in isolated protoplasts, the fusion protein efficiently targeted to the membrane of the large central vacuole, the lytic compartment of plant cells. Membrane currents recorded from EGFP-positive vacuoles were almost voltage independent and showed time-dependent activation at elevated positive membrane potentials as a hallmark. The shift in the reversal potential of the current induced by a decrease of cytosolic pH was compatible with a $2Cl^-/1H^+$ exchange stoichiometry. Mutating the so-called gating glutamate into alanine (E245A) uncoupled chloride fluxes from the movement of protons, transforming the transporter into a chloride channel-like protein. Importantly, CLC-7 transport activity in the vacuolar expression system was recorded in the absence of the auxiliary subunit Ostm1, differently to recent data obtained in *Xenopus* oocytes using a CLC-7 mutant with partial plasma membrane expression. We also show that plasma membrane-targeted $CLC\text{-}7_{E245A}$ is non-functional in *Xenopus* oocytes when expressed without Ostm1. In summary, our data suggest the existence of an alternative CLC-7 operating mode, which is active when the protein is not in complex with Ostm1. The

A. Costa, P. V. K. Gutla and A. Boccaccio contributed equally to this work.

DOI: 10.1113/jphysiol.2012.230227

vacuolar expression system has the potential to become a valuable tool for functional studies on intracellular ion channels and transporters from animal cells.

(Received 20 March 2012; accepted after revision 25 May 2012; first published online 28 May 2012)
Corresponding author A. Carpaneto: Armando Carpaneto, Istituto di Biofisica-CNR, Via De Marini 6, 16149 Genova, Italy. Email: carpaneto@ge.ibf.cnr.it

Abbreviations CLC, chloride channel; EGFP, enhanced green fluorescent protein; Ostm1, osteopetrosis-associated transmembrane protein 1; V_{rev}, reversal voltage.

Introduction

Intracellular ion channels and transporters of animal cells have become a centre of interest, as they play important roles in many physiological and pathological processes. However, this large group of proteins is still largely unexplored. There is a lack of information on their basic functional properties such as selectivity, turnover rate, voltage dependence and pharmacology, primarily because of their intracellular localization, which represents a major obstacle for a detailed functional characterization based on standard electrophysiological techniques.

Mammalian CLC-7 protein is a broadly expressed member of the ClC family of chloride transporters residing in late endosomes and lysosomes as well as in the ruffled border of bone-resorbing osteoclasts (Kasper *et al.* 2005). The association with the membrane protein Ostm1 appears to be essential for CLC-7 protein stability in mammals (Lange *et al.* 2006). The CLC-7–Ostm1 molecular complex is thought to provide an anion conductance for lysosomal chloride accumulation or neutralization of proton pump-mediated currents. In line with this, loss of either *Clcn7* or *Ostm1* gene function lead to similar pathologies comprising osteopetrosis, lysosomal storage disease and neuronal degeneration in humans and mice (Kornak *et al.* 2001; Chalhoub *et al.* 2003; Kasper *et al.* 2005; Lange *et al.* 2006). Recent efforts using different experimental approaches have produced first insights in CLC-7 function and its interaction with the Ostm1 β-subunit. Flux measurements of radioactive chloride in native lysosomes purified from rat liver provided the first evidence for chloride/proton antiport activity of CLC-7 (Graves *et al.* 2008). Applying solid-supported membrane-based electrophysiology to lysosomal membrane fractions from CLC-7:EGFP-expressing Chinese hamster ovary (CHO) cells, Schulz *et al.* (2010) recorded pH- and anion-dependent transient currents. Ostm1 co-expression appeared to increase the amount of CLC-7:EGFP and the measured currents in this system. Finally, the creation of a CLC-7 mutant with partial plasma membrane targeting (LL23/24AA, LL36/37AA; CLC-7^{PM}), following the identification of lysosomal sorting motifs (Stauber & Jentsch, 2010), allowed voltage-clamp recordings of CLC-7-dependent currents in mammalian cell lines and *Xenopus* oocytes to be made (Leisle *et al.* 2011), which until then were bound to fail (Brandt & Jentsch, 1995; Schulz *et al.* 2010). Intriguingly, CLC-7^{PM} was only functional when co-expressed with its β-subunit Ostm1. CLC-7/Ostm1 currents showed strong voltage-dependent outward rectification and slow time courses of activation and deactivation. Reversal potential shifts were in agreement with $2Cl^-/1H^+$ antiport activity (Leisle *et al.* 2011).

Here, we studied CLC-7 transport activity in isolated vacuoles of *Arabidopsis thaliana* leaf cells. The central lytic vacuole can be regarded as the plant counterpart of the animal lysosome, even though it fulfills many more functions, e.g. in ion and pH homeostasis and turgor regulation of the plant cell. In many cell types, this large compartment (up to 40 μm in diameter) occupies more than 80% of the cellular volume (Marty, 1999; Martinoia *et al.* 2007). Simplicity of isolation and its large size make it a highly convenient system for patch-clamp studies. Consequently, many types of endogenous ion channels and transporters have been identified and characterized in great detail (Martinoia *et al.* 2007). We show that overexpression in transiently transformed mesophyll protoplasts lead to massive incorporation of functional CLC-7 into the vacuolar membrane. The current characteristics indicated chloride/proton antiport activity of vacuolar CLC-7, but they also revealed novel features regarding the voltage dependence and Ostm1 requirement of CLC-7.

Methods

DNA constructs

For protoplast expression, the coding sequences of the *Rattus norvegicus* chloride channel 7 (rCLC-7) or rCLC-7_{E245A} were PCR-amplified using the Phusion DNA polymerase (Finnzymes, http://www.finnzymes.fi/). The forward primer 5′-CATGAAGCTTCATGGCCAACGTT TCTAAGAAAGTGTCT-3′ and the reverse primer 5′-CATGGAATTCCGTCTGGGCCAGTGAAAGCTCTTC T-3′ contained HindIII and EcoRI restriction sites, respectively, which were used for the subcloning into the plant expression vector pSAT6-EGFP-N1 (Tzfira *et al.*

2005), downstream of the double cauliflower mosaic virus 35S promoter and upstream of the EGFP coding sequence.

For oocyte expression, the E245A mutant of rCLC-7 was introduced into the background of N-terminal mutant L23A/L24A/L/36A/L37A to increase surface expression (Stauber & Jentsch, 2010; Leisle *et al.* 2011) and cloned into the PTLN vector (Lorenz *et al.* 1996). In a second construct, the E^2GFP-DsRed chloride/pH sensor (Arosio *et al.* 2010) was fused to the C-terminus. Mouse Ostm1 was in pFROG, a pCDNA3-derived vector suitable for expression in *Xenopus* oocytes. Mutants were generated by PCR and sequenced.

Plant material and protoplast transformation

Plants of *Arabidopsis thaliana* (wild-type strain Columbia-0; *Atclca* knock-out) were grown in soil in a growth chamber at 22°C and with an 8 h light–16 h dark regime.

Mesophyll protoplasts were isolated and transiently transformed according to a well-established protocol (Yoo *et al.* 2007). Briefly, well-expanded rosette leaves from 3- to 5-week-old plants were cut into strips of 0.5–1 mm with a fresh razor blade. Leaf tissue was digested in enzyme solution containing 1% cellulase and 0.2% macerozyme for 3 h at 23°C. The protoplast suspension was filtered through a 50 μm nylon mesh and used for PEG transfection at a density of 2×10^5 cells ml^{-1}. Protoplasts were maintained in ionic solution W5 (in mM: 125 $CaCl_2$, 154 NaCl, 5 KCl, 2 Mes-KOH, pH 5.6, ampicillin 50 $\mu g\,ml^{-1}$) for 2–4 days at 23°C in the dark. Vacuoles were released from protoplasts by perfusion with standard patch-clamp bath solution (see below). Alternatively, efficient vacuole release was achieved by mixing 1 volume of a protoplast aliquot with 10 volumes of vacuole release solution (in mM: 100 malic acid, 1,3-*bis*(tris(hydroxymethyl)methylamino)propane (BTP), 5 EGTA, 3 $MgCl_2$, pH 7.5, 450 mOsm with D-sorbitol). The transformation efficiency judged by GFP fluorescence in protoplasts was routinely 50–70%, and in 60–80% of transformed protoplasts GFP fluorescence was detected at the vacuolar membrane.

A schematic overview of the heterologous expression of intracellular animal channels and transporters in isolated vacuoles from plant cells is presented in Supplemental Fig. S1.

Patch-clamp recordings on mesophyll vacuoles

Approximately 40 h after protoplast transformation, patch-clamp experiments were performed on isolated vacuoles. CLC-7-containing vacuoles were identified by EGFP fluorescence. Patch pipettes were pulled from thin-walled borosilicate glass (Harvard Apparatus Ltd, Kent, UK). Ionic currents were recorded with a List EPC7 current–voltage amplifier. Data were digitized using a 16-bit Instrutech A/D/A board (Instrutech, Elmont, NY, USA) interfaced to a MacIntosh PC, which generated the voltage stimulation protocol and archived the current response.

The standard pipette (vacuolar side) solution contained (in mM): 200 HCl, 105 BTP, 1 $CaCl_2$, 5 $MgCl_2$, 5 2-(*N*-morpholino)ethanesulfonic acid (Mes), pH 5.5. The standard bath (cytoplasmic side) solution contained (in mM): 15 HCl, 18 BTP, 0.1 $CaCl_2$, 2 $MgCl_2$, 2 dithiothreitol (DTT), 15 Mes, pH 7.0. The bath solution at pH 5.7 contained 10 mM BTP. High-chloride bath solution contained 200 mM HCl and 140 mM BTP. The osmolarity of the vacuolar and cytoplasmic solution was adjusted to 600 mOsm and 650 mOsm, respectively, by the addition of D-sorbitol. The whole-vacuole configuration was achieved by simultaneously applying a voltage pulse (700 mV, 0.7 ms duration) and slight suction (about –10 mmHg). Recordings were started after stabilization of the currents, generally about 4 min after break-in. According to the convention regarding electrical measurements on endomembranes (Bertl *et al.* 1992), positive currents correspond to anions flowing from the lumen of the vacuole to the cytoplasmic side or cations moving in the opposite direction (for a schematic representation of the whole-vacuole configuration see Supplemental Fig. S2). The liquid junction potential between the standard pipette and bath solutions was 26.8 ± 0.3 mV ($n = 10$) and was subtracted off-line. Steady-state current amplitudes were normalized to the vacuolar membrane capacitance, ranging from 15 to 80 pF. Time-dependent activation of control and CLC-7:EGFP currents was evaluated by subtracting the mean current after the capacitative transient at the beginning of the voltage pulse from the steady-state current. Chemicals were purchased from Sigma (Milan, Italy).

Two-electrode voltage-clamp on *Xenopus* oocytes

In accordance with national guidelines, oocytes were collected from *Xenopus* females anaesthetized with tricaine. After surgery, frogs were allowed to recover from anaesthesia and suitable aftercare was given. Frogs were used two or three times for oocyte harvesting, allowing for at least 2 months of recovery between the operations. After the final operation, frogs were deeply anaesthetized and then killed by decapitation in agreement with the standards of *The Journal of Physiology* (http://jp.physoc.org/content/587/4/713.full.pdf&±html). Expression in *Xenopus* oocytes and two-electrode voltage-clamp recordings were performed as described in Gradogna *et al.* (2010).

The standard extracellular solution contained (in mM): 100 NaCl, 5 $MgSO_4$, 10 Hepes, pH 7.3. Chloride concentration was changed by substitution of NaCl with sodium glutamate. For all recordings, the pulse protocol consisted of voltage steps of 100 ms from –140 to +60 mV with +20 mV increments from a holding potential of –20 mV, preceded by a 50 ms conditioning prepulse to +60 mV and followed by a 50 ms postpulse to –100 mV.

Data analysis

All data throughout text and figures are reported as means ± SEM. Data analysis was performed with IgorPro software (Wavemetrics, Lake Oswego, OR, USA) or with the custom analysis program Ana (freely available at http://users.ge.ibf.cnr.it/pusch/). Figures were prepared using IgorPro software.

Results

CLC-7:EGFP fusion protein localizes to the vacuolar membrane of transiently transformed *Arabidopsis* mesophyll protoplasts

Mesophyll protoplasts isolated from *Arabidopsis thaliana* wild-type leaves (ecotype Columbia-0) were transiently transformed with a plasmid carrying a CLC-7:EGFP fusion under the control of the strong constitutive cauliflower mosaic virus 35S promoter. After the incubation period, protoplast lysis was induced by perfusion of the recording chamber with standard bath solution used in patch-clamp recordings (see Methods and Supplemental Fig. S1). This procedure allowed release of the cellular contents without damaging the large central vacuole (Fig. 1*A*). Red fluorescence signals in Fig. 1*B* indicate the autofluorescence of isolated chloroplasts. Transformed protoplasts showed strong GFP fluorescence at the vacuolar membrane (Fig. 1*C* and *D*), demonstrating that the CLC-7:EGFP fusion protein was efficiently targeted to the central vacuole.

CLC-7:EGFP encodes a functional anion transport protein in *Arabidopsis* vacuoles

To test if the CLC-7:EGFP protein in the vacuolar membrane was functional, we performed patch-clamp experiments on isolated fluorescent vacuoles. The genetic background of the *Atclca* knock-out mutant was chosen for these measurements, in order to avoid a possible interference by ClCa, a highly expressed anion/proton antiporter in *Arabidopsis* mesophyll cells (De Angeli *et al.* 2006). Expression level and vacuolar localization in *Atclca* plants were identical to *Arabidopsis* wild-type plants (data not shown). Membrane currents of CLC-7:EGFP-containing vacuoles (Fig. 2*A*, middle panel) were significantly larger than those of non-transformed control vacuoles (Fig. 2*A*, left panel), especially at positive membrane potentials. The *I–V* plot showed slight outward rectification for CLC-7:EGFP currents (Fig. 2*B*; open circles) and the reversal potential (V_{rev}) of -13.4 ± 1.4 mV ($n = 26$) was far from the Nernst potentials for chloride ($E_{Cl} = -61.1$ mV) and protons ($E_H = +87.8$ mV) or any other ion in the experimental solutions, but in accordance with $2Cl^-/1H^+$ exchange activity (–11.5 mV). In contrast, the reversal potential of control currents was considerably more negative (-26.1 ± 3.3 mV, $n = 30$; Fig. 2*B*, filled triangles). The slope conductance at the reversal potential was 18.5 ± 2.0 pS pF^{-1} for CLC-7:EGFP recordings ($n = 26$) and significantly different from 8.3 ± 0.9 pS pF^{-1} for control vacuoles ($n = 30$; $P < 0.001$; unpaired Student's *t* test). Furthermore, CLC-7:EGFP currents exhibited time-dependent activation at membrane potentials above +50 mV, a hallmark characteristic which was not observed in control currents (Fig. 2*C* and inset therein).

Mutational studies have shown that a conserved glutamate residue within the selectivity filter is necessary for the coupling mechanism between anion and proton fluxes in antiporters of the ClC family (Dutzler *et al.* 2003; Accardi *et al.* 2005; Picollo & Pusch, 2005; Bergsdorf *et al.* 2009; Leisle *et al.* 2011). Transient expression of a CLC-7 version bearing a substitution of

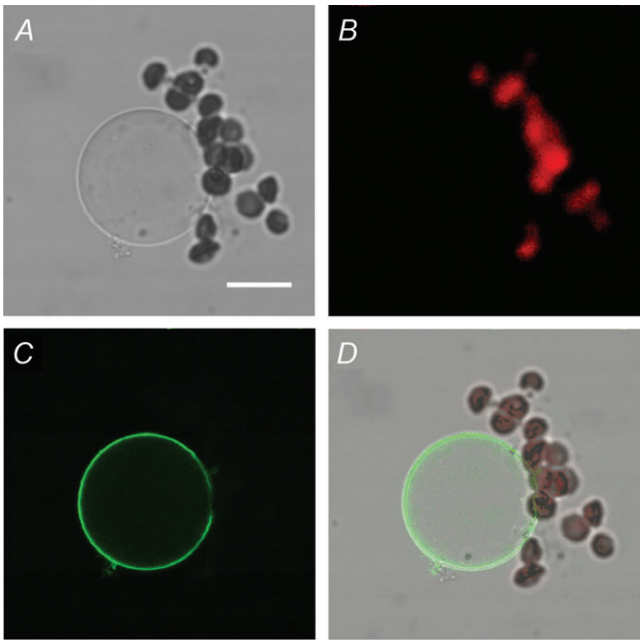

Figure 1. Vacuolar localization of CLC-7:EGFP in *Arabidopsis* mesophyll protoplasts *A–D*, confocal images of a representative vacuole isolated by lysis of a CLC-7:EGFP-expressing protoplast. *A*, bright field; *B*, red chlorophyll autofluorescence of isolated chloroplasts; *C*, green fluorescence of CLC-7:EGFP at the vacuolar membrane; *D*, overlay. Scale bar, 7 μm.

the 'gating glutamate' with alanine (CLC-7_{E245A}:EGFP) yielded time-independent currents with large amplitudes (about 4-fold at $V_m = +93$ mV) and a reversal potential of -43.7 ± 1.9 mV ($n = 10$), in agreement with a passive chloride conductance (Fig. 2*A*, right panel; Fig. 2*D*, filled squares).

Next, we investigated if CLC-7:EGFP currents responded to pH changes, as expected from a proton-coupled chloride antiporter. Changing the pH of the bath solution from 7 to 5.7 caused the currents of CLC-7:EGFP-containing vacuoles to become more positive at all membrane potentials (Fig. 3*A*). The shift of the reversal potential by -19.2 ± 1.6 mV ($n = 13$) was again in good agreement with the theoretical value ($\Delta V_{rev} = -25.4$ mV) expected for a $2Cl^-/1H^+$ antiport mechanism. Accordingly, cytosolic acidification caused the largest current increase at positive potentials, corresponding to enhanced chloride flux from the vacuolar lumen to the bath. In contrast, CLC-7_{E245A}:EGFP vacuoles exposed to pH 5.7 neither displayed increased positive currents nor a negative shift of the reversal potential (Fig. 3*B*), confirming the uncoupling of chloride and proton fluxes in this mutant. The channel-like behaviour of CLC-7_{E245A}:EGFP was further highlighted by experiments in which the trans-membrane chloride gradient was abolished by increasing the chloride concentration in the bath solution from 19 mM to 200 mM. CLC-7_{E245A}:EGFP currents reversibly decreased at positive potentials and increased at negative ones, shifting the reversal potential close to the theoretical Nernst potential for chloride (Fig. 4*A* and *B*).

Taken together, these data demonstrated that CLC-7 – both the wild-type and E245A mutant form – constitutes a functional transport protein in *Arabidopsis* vacuoles. Its abundant expression in transiently transformed protoplasts ensured that it dominated the ionic

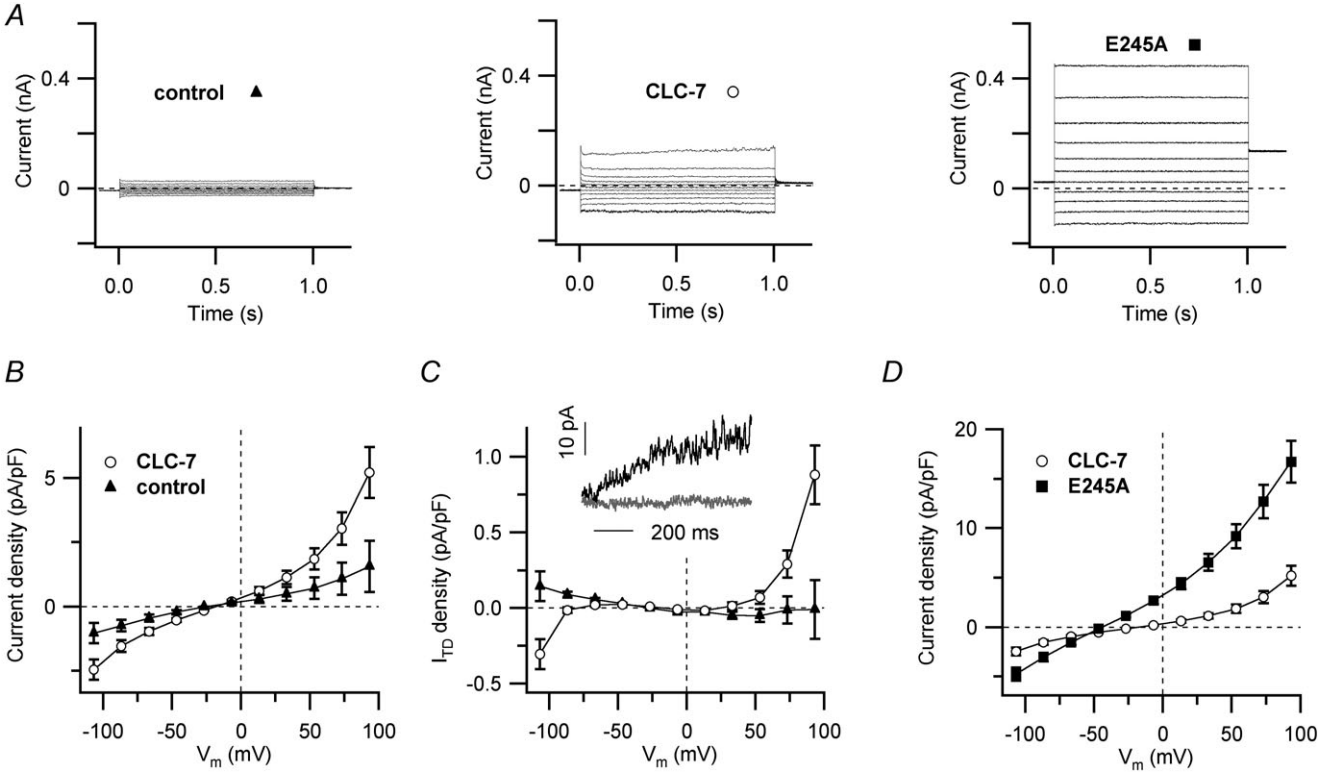

Figure 2. Patch-clamp recordings on isolated vacuoles from transiently transformed *Arabidopsis* mesophyll protoplasts
A, macroscopic currents elicited by a series of voltage steps ranging from –107 to +93 mV in +20 mV steps and recorded from control vacuoles (left panel), from vacuoles containing CLC-7:EGFP (CLC-7; middle panel) or CLC-7_{E245A}:EGFP (E245A; right panel). The holding and tail potentials were –27 mV and +23 mV, respectively. *B*, average steady-state currents of control (filled triangles; $n = 30$) and CLC-7:EGFP vacuoles (open circles; $n = 26$) were normalized to the vacuolar capacitance and plotted *vs.* membrane potential. *C*, mean values of time-dependent current density (I_{TD} density, see Methods) were plotted *vs.* membrane potential. In the inset, raw data recorded at +93 mV in control (grey trace) and in a CLC-7:EGFP-containing vacuole (black trace) from the experiments in *A* are shown. For better comparison, the traces were shifted to the same initial value. *D*, average steady-state current densities of CLC-7:EGFP (as in *B*) and CLC-7_{E245A}:EGFP vacuoles (filled squares; $n = 10$) were plotted *vs.* membrane potential. Data points represent mean ± SEM.

conductance of the vacuolar membrane, as emphasized by the current amplitudes and reversal potentials. Importantly, the current characteristics reported here are in good agreement with chloride–proton exchange activity of CLC-7, as described previously in other experimental systems.

CLC-7_{E245A} requires the β-subunit Ostm1 for transport activity in *Xenopus* oocytes

It is important to emphasize that, in the vacuolar expression system, CLC-7-dependent currents were detectable in the absence of the auxiliary subunit Ostm1. Conversely, in *Xenopus* oocytes expressing a CLC-7 mutant with partial plasma membrane targeting (CLC-7^{PM}), transport activity was obtained exclusively with Ostm1 co-expression (Leisle *et al.* 2011). Although CLC-7^{PM} reached the plasma membrane in oocytes, it appeared to be inactive without Ostm1. In this context, we investigated the Ostm1 requirement of the E245A mutant in *Xenopus* oocytes. Expression of CLC-$7^{PM}{}_{E245A}$ without Ostm1 yielded no currents (Fig. 5*A*, left panel), while Ostm1 co-expression elicited large, time- and voltage-independent currents (Fig. 5*A*, middle panel; Leisle *et al.* 2011). Complete removal of extracellular chloride suppressed the outwardly directed current component (Fig. 5*A*, right panel) and shifted the reversal

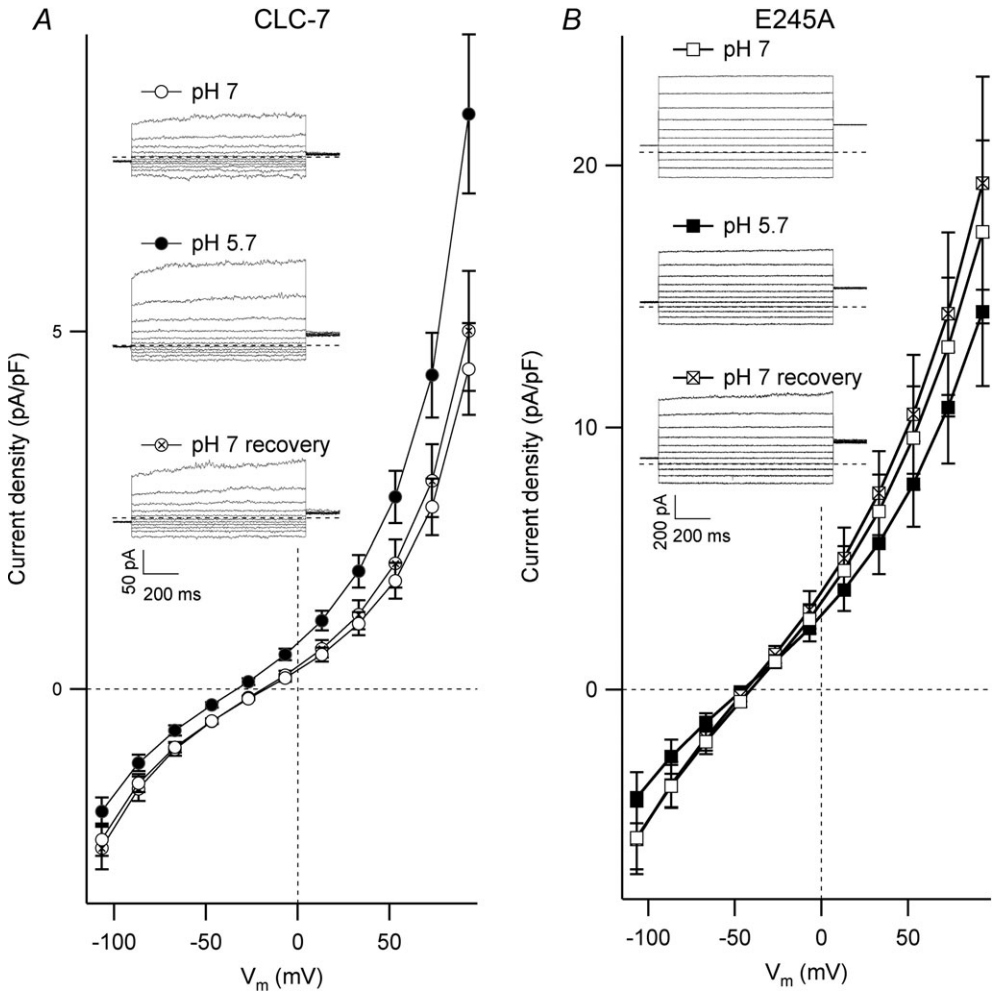

Figure 3. CLC-7 and CLC-7_{E245A} currents in *Arabidopsis* vacuoles show differential sensitivity to cytosolic pH
Average steady-state current densities recorded from vacuoles containing CLC-7:EGFP (*A*) or CLC-7_{E245A}:EGFP (*B*) were plotted *vs.* membrane potential. Macroscopic currents were elicited by a series of voltage steps ranging from –107 to +93 mV in +20 mV steps; representative current traces are shown in the insets. Cytosolic pH sensitivity was tested by changing the bath solution from pH 7 (top panels; recovery in bottom panels) to pH 5.7 (middle panels). The holding potential was –27 mV. The reversal potential of CLC-7:EGFP currents (*A*; $n = 13$) shifted reversibly from –15.8 ± 1.8 mV at pH 7 to –35.0 ± 1.4 mV at pH 5.7. The reversal potential of CLC-7_{E245A}:EGFP currents (*B*; $n = 4$) was –41.1 ± 2.0 mV at pH 7 and –46.0 ± 1.2 mV at pH 5.7. Data points represent mean ± SEM.

potential to more positive values (Fig. 5*B*), as expected from a chloride-selective current. In these experiments, a fluorescent reporter protein (E^2GFP-DsRed; Arosio *et al.* 2010) was C-terminally fused to CLC-7^{PM}_{E245A}. The presence of the fusion protein did not interfere with CLC-7^{PM}_{E245A} function, since identical results were obtained with CLC-7^{PM}_{E245A} alone (data not shown). In summary, these results demonstrated that CLC-7^{PM} and CLC-7^{PM}_{E245A} do not differ in their Ostm1 requirement for transport activity in *Xenopus* oocytes.

Discussion

In this study, we used mesophyll protoplasts of the model plant *Arabidopsis thaliana* as a novel heterologous expression system for the lysosomal chloride/proton exchanger CLC-7 from rat. CLC-7:EGFP fusion protein targeted efficiently to the central lytic vacuole of transiently transformed protoplasts. Expression of CLC-7:EGFP in the genetic background of *Atclca* knock-out plants yielded vacuolar currents with higher amplitudes than control vacuoles and with the characteristics of chloride/proton antiport: reversal potential measurements at pH 7 and pH 5.7 were in accordance with a $2Cl^-/1H^+$ exchange stoichiometry, as reported previously (Leisle *et al.* 2011). Intriguingly, CLC-7:EGFP currents in the vacuolar membrane differed in three major properties from the currents recorded in *Xenopus* oocytes expressing CLC-7^{PM}, a mutant with partial plasma membrane targeting (Leisle *et al.* 2011): (i) CLC-7:EGFP currents appeared to be active

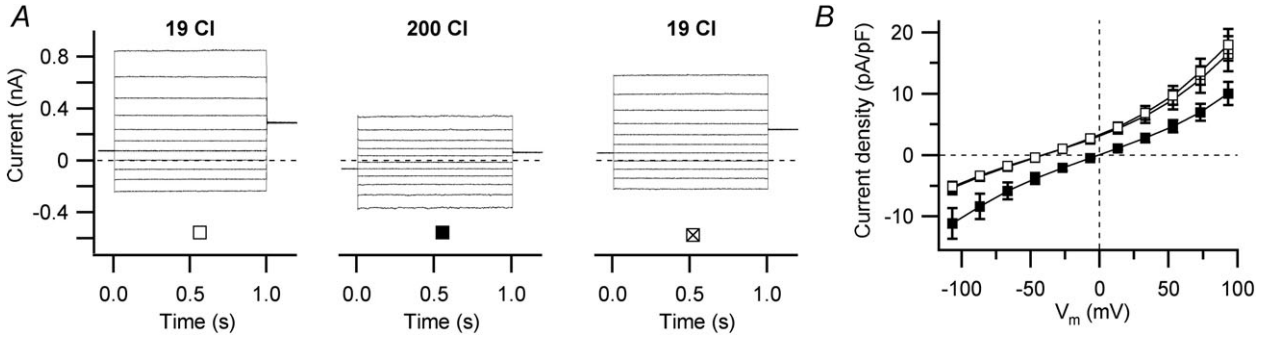

Figure 4. Chloride channel-like behaviour of CLC-7_{E245A} in *Arabidopsis* vacuoles
A, macroscopic currents elicited by a series of voltage steps ranging from –107 to +93 mV in +20 mV steps and recorded from vacuoles containing CLC-7_{E245A}:EGFP. The chloride concentration of the bath solution was changed from 19 mM (left panel; recovery in right panel) to 200 mM (middle panel). The holding potential was –27 mV. *B*, average steady-state current densities ($n = 6$) were plotted *vs.* membrane potential. The reversal potential reversibly shifted from –40.3 ± 2.1 mV in 19 mM Cl^- (open squares) to –0.2 ± 0.9 mV in 200 mM Cl^- (filled squares). Data points represent mean ± SEM.

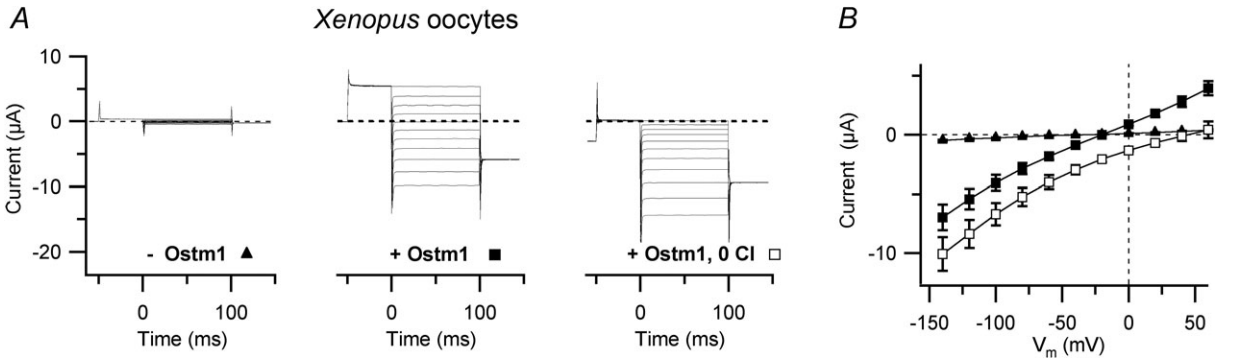

Figure 5. CLC-7_{E245A} requires Ostm1 for transport activity in *Xenopus* oocytes
A, two-electrode voltage-clamp recordings on *Xenopus* oocytes expressing CLC-7^{PM}_{E245A}:E^2GFP-DsRed (left panel) or CLC-7^{PM}_{E245A}:E^2GFP-DsRed + Ostm1 (middle panel) in standard bath solution with 100 mM chloride. The right panel shows CLC-7^{PM}_{E245A}:E^2GFP-DsRed + Ostm1 currents after removal of extracellular chloride (0 Cl). Currents were elicited by a pre-pulse to +60 mV followed by test potentials ranging from –140 to +60 mV in +20 mV steps, from a holding potential of –20 mV. *B*, average steady-state currents in oocytes expressing CLC-7^{PM}_{E245A}:E^2GFP-DsRed alone ($n = 8$; filled triangles) or together with Ostm1 ($n = 12$; filled squares) in standard bath solution. Open squares represent average currents of CLC-7^{PM}_{E245A}:E^2GFP-DsRed + Ostm1 in 0 Cl bath solution ($n = 12$). Data points represent mean ± SEM.

in the full range of membrane potentials, showing only slight outward rectification; (ii) CLC-7:EGFP currents displayed only small time-dependent activation kinetics at positive potentials, but no detectable tail currents; (iii) CLC-7:EGFP currents were recorded in the absence of the β-subunit Ostm1. One might argue that the role played by Ostm1 in animal cells concerning the stabilization and activation of CLC-7 could be taken over by an endogenous protein present in the *Arabidopsis* vacuole. BLAST searches argue against this possibility as they did not reveal sequence homologies to Ostm1 in the *Arabidopsis thaliana* genome in particular and in plant genomes in general. Furthermore, CLC-7 might be stabilized by heteromeric interactions with endogenous members of the ClC family. However, co-immunoprecipitation studies in transfected HEK cells indicated that CLC-7 transporters are likely to be homomeric (Suzuki *et al.* 2006). Most importantly, patch-clamp experiments on CLC-7:EGFP were conducted in the *Atclca* knock-out mutant, i.e. in the absence of the predominantly expressed isoform in mesophyll protoplasts. Other vacuolar CLC proteins are present in too low amounts to enable heteromer formation with overexpressed CLC-7:EGFP in a quantitive manner (see Arabidopsis eFP Browser at http://bar.utoronto.ca/efp/cgi-bin/efpWeb.cgi).

CLC-7 transport activity in the vacuolar membrane was further supported by experiments on CLC-7_{E245A}:EGFP-containing vacuoles. Mutation of the 'gating glutamate' transformed CLC-7 from a proton-coupled antiporter into a passive chloride conductance. These data were entirely analogous to those obtained with CLC-7^{PM}_{E245A}/Ostm1 in *Xenopus* oocytes (Leisle *et al.* 2011). However, as shown in the present study, CLC-7^{PM}_{E245A} expressed without Ostm1 did not produce detectable currents in oocytes. One can only speculate on the reasons for this divergent behaviour between the vacuole and oocyte systems. The amino acid substitutions responsible for the plasma membrane targeting of CLC-7^{PM} may render the protein non-functional in the absence of Ostm1. Alternatively, it may be caused by differences determined by the experimental system, e.g. the lipid composition of the membrane, the cytoskeleton or other cytosolic factors.

Taken together, our data suggest the existence of an alternative operating mode of CLC-7, in addition to the previously reported time- and voltage-activated characteristics of the CLC-7/Ostm1 molecular complex (Leisle *et al.* 2011). A fraction of CLC-7 in animal lysosomes may be active without the β-subunit Ostm1 allowing the exchanger to be active at all membrane potentials.

The functional characterization of lysosomal/endosomal ion channels and transporters from animal cells generally suffers from the inaccessibility of endomembranes to standard electrophysiological techniques. Alternative approaches have been devised to elucidate aspects of transporter function in small organelles. Purified native lysosomes were employed in flux measurements (Graves *et al.* 2008) and solid-supported membrane-based electrophysiology (Schulz *et al.* 2010). Enlarged lysosomes were obtained by vacuolin-1 treatment and used in voltage-clamp experiments to study the lysosomal channels TRPML1 (Dong *et al.* 2008) and TPCN2 (Schieder *et al.* 2010). With an average membrane capacitance of less than 0.4 pF, enlarged lysosomes are not suited to the detection of transporter-mediated currents, which have typical current densities of 10–20 pA pF^{-1} (Hille, 2001). Incorporation into liposomes or artificial membranes, as done for TPCN2 (Pitt *et al.* 2010), requires the purification of sufficient amounts of recombinant protein and lacks control of the protein orientation within the membrane. Finally, by manipulation of N-terminal sorting signals in CLC-6 (Neagoe *et al.* 2010) and CLC-7 (Leisle *et al.* 2011), these endosomal CLC proteins were partially targeted to the plasma membrane and became accessible to patch-clamp experiments.

In this study on CLC-7, we propose the central lytic vacuole of *Arabidopsis* mesophyll protoplasts as a novel system for the functional characterization of intracellular transporters from animal cells. This large organelle constitutes a convenient system for detailed patch-clamp studies (Hedrich, 1995; Hedrich & Marten, 2006). In addition to macroscopic current recordings from the whole vacuole, many reports investigated single channel behaviour and modulation in excised vacuolar membrane patches, both in the cytosolic-side-out (Scholz-Starke *et al.* 2006) and vacuolar-side-out configurations (Pottosin & Martinez-Estevez, 2003). Furthermore, fluorescent indicator dyes have been employed in combination with the patch-clamp technique (Konrad & Hedrich, 2008; Gradogna *et al.* 2009). Despite the presence of diverse types of endogenous ion transport systems, the density of background currents can be significantly reduced by the choice of ionic conditions and/or the use of appropriate *Arabidopsis* knock-out lines. In the present study, we used a knock-out line lacking the highly expressed AtCLCa transporter (De Angeli *et al.* 2006), in order to determine CLC-7-dependent activity in conditions of low current background. A further, unique advantage of this experimental system lies in the fact that in the whole-vacuole configuration the cytosolic side of the membrane faces the external bath solution, which makes it ideal to investigate the effects of cytosolic compounds like second messengers, activators and blockers (De Angeli *et al.* 2009). The results presented here suggest that the vacuolar expression system has the potential to become a reference system for functional studies on transport systems from animal endomembranes.

References

Accardi A, Walden M, Nguitragool W, Jayaram H, Williams C & Miller C (2005). Separate ion pathways in a Cl^-/H^+ exchanger. *J Gen Physiol* **126**, 563–570.

Arosio D, Ricci F, Marchetti L, Gualdani R, Albertazzi L & Beltram F (2010). Simultaneous intracellular chloride and pH measurements using a GFP-based sensor. *Nat Methods* **7**, 516–518.

Bergsdorf EY, Zdebik AA & Jentsch TJ (2009). Residues important for nitrate/proton coupling in plant and mammalian CLC transporters. *J Biol Chem* **284**, 11184–11193.

Bertl A, Blumwald E, Coronado R, Eisenben R, Firlay G, Gradmann D, Hille B, Kohler K, Koll HA, MacRobbie E, Meissner G, Miller C, Neher E & Palade P (1992). Electrical measurements on endomembranes. *Science* **258**, 873–874.

Brandt S & Jentsch TJ (1995). CLC-6 and CLC-7 are two novel broadly expressed members of the CLC chloride channel family. *FEBS Lett* **377**, 15–20.

Chalhoub N, Benachenhou N, Rajapurohitam V, Pata M, Ferron M, Frattini A, Villa A & Vacher J (2003). Grey-lethal mutation induces severe malignant autosomal recessive osteopetrosis in mouse and human. *Nat Med* **9**, 399–406.

De Angeli A, Monachello D, Ephritikhine G, Frachisse JM, Thomine S, Gambale F & Barbier-Brygoo H (2006). The nitrate/proton antiporter AtCLCa mediates nitrate accumulation in plant vacuoles. *Nature* **442**, 939–942.

De Angeli A, Moran O, Wege S, Filleur S, Ephritikhine G, Thomine S, Barbier-Brygoo H & Gambale F (2009). ATP binding to the C terminus of the Arabidopsis thaliana nitrate/proton antiporter, AtCLCa, regulates nitrate transport into plant vacuoles. *J Biol Chem* **284**, 26526–26532.

Dong XP, Cheng X, Mills E, Delling M, Wang F, Kurz T & Xu H (2008). The type IV mucolipidosis-associated protein TRPML1 is an endolysosomal iron release channel. *Nature* **455**, 992–996.

Dutzler R, Campbell EB & MacKinnon R (2003). Gating the selectivity filter in ClC chloride channels. *Science* **300**, 108–112.

Gradogna A, Babini E, Picollo A & Pusch M (2010). A regulatory calcium-binding site at the subunit interface of CLC-K kidney chloride channels. *J Gen Physiol* **136**, 311–323.

Gradogna A, Scholz-Starke J, Gutla PV & Carpaneto A (2009). Fluorescence combined with excised patch: measuring calcium currents in plant cation channels. *Plant J* **58**, 175–182.

Graves AR, Curran PK, Smith CL & Mindell JA (2008). The Cl^-/H^+ antiporter CLC-7 is the primary chloride permeation pathway in lysosomes. *Nature* **453**, 788–792.

Hedrich R (1995). Technical approaches to studying specific properties of ion channels in plants. In *Single Channel Recordings*, ed. Sakmann B & Neher E. Plenum Press, New York and London.

Hedrich R & Marten I (2006). 30-year progress of membrane transport in plants. *Planta* **224**, 725–739.

Hille B (2001). *Ionic Channels of Excitable Membranes*. Sinauer Ass. Inc., Sunderland, MA.

Kasper D, Planells-Cases R, Fuhrmann JC, Scheel O, Zeitz O, Ruether K, Schmitt A, Poet M, Steinfeld R, Schweizer M, Kornak U & Jentsch TJ (2005). Loss of the chloride channel CLC-7 leads to lysosomal storage disease and neurodegeneration. *EMBO J* **24**, 1079–1091.

Konrad KR & Hedrich R (2008). The use of voltage-sensitive dyes to monitor signal-induced changes in membrane potential-ABA triggered membrane depolarization in guard cells. *Plant J* **55**, 161–173.

Kornak U, Kasper D, Bosl MR, Kaiser E, Schweizer M, Schulz A, Friedrich W, Delling G & Jentsch TJ (2001). Loss of the CLC-7 chloride channel leads to osteopetrosis in mice and man. *Cell* **104**, 205–215.

Lange PF, Wartosch L, Jentsch TJ & Fuhrmann JC (2006). CLC-7 requires Ostm1 as a beta-subunit to support bone resorption and lysosomal function. *Nature* **440**, 220–223.

Leisle L, Ludwig CF, Wagner FA, Jentsch TJ & Stauber T (2011). CLC-7 is a slowly voltage-gated $2Cl^-/1H^+$-exchanger and requires Ostm1 for transport activity. *EMBO J* **30**, 2140–2152.

Lorenz C, Pusch M & Jentsch TJ (1996). Heteromultimeric CLC chloride channels with novel properties. *Proc Natl Acad Sci U S A* **93**, 13362–13366.

Martinoia E, Maeshima M & Neuhaus HE (2007). Vacuolar transporters and their essential role in plant metabolism. *J Exp Bot* **58**, 83–102.

Marty F (1999). Plant vacuoles. *Plant Cell* **11**, 587–600.

Neagoe I, Stauber T, Fidzinski P, Bergsdorf EY & Jentsch TJ (2010). The late endosomal CLC-6 mediates proton/chloride countertransport in heterologous plasma membrane expression. *J Biol Chem* **285**, 21689–21697.

Picollo A & Pusch M (2005). Chloride/proton antiporter activity of mammalian CLC proteins CLC-4 and CLC-5. *Nature* **436**, 420–423.

Pitt SJ, Funnell TM, Sitsapesan M, Venturi E, Rietdorf K, Ruas M, Ganesan A, Gosain R, Churchill GC, Zhu MX, Parrington J, Galione A & Sitsapesan R (2010). TPC2 is a novel NAADP-sensitive Ca^{2+} release channel, operating as a dual sensor of luminal pH and Ca^{2+}. *J Biol Chem* **285**, 35039–35046.

Pottosin II & Martinez-Estevez M (2003). Regulation of the fast vacuolar channel by cytosolic and vacuolar potassium. *Biophys J* **84**, 977–986.

Schieder M, Rotzer K, Bruggemann A, Biel M & Wahl-Schott CA (2010). Characterization of two-pore channel 2 (TPCN2)-mediated Ca^{2+} currents in isolated lysosomes. *J Biol Chem* **285**, 21219–21222.

Scholz-Starke J, Carpaneto A & Gambale F (2006). On the interaction of neomycin with the slow vacuolar channel of Arabidopsis thaliana. *J Gen Physiol* **127**, 329–340.

Schulz P, Werner J, Stauber T, Henriksen K & Fendler K (2010). The G215R mutation in the Cl^-/H^+-antiporter CLC-7 found in ADO II osteopetrosis does not abolish function but causes a severe trafficking defect. *PLoS One* **5**, e12585.

Stauber T & Jentsch TJ (2010). Sorting motifs of the endosomal/lysosomal CLC chloride transporters. *J Biol Chem* **285**, 34537–34548.

Suzuki T, Rai T, Hayama A, Sohara E, Suda S, Itoh T, Sasaki S & Uchida S (2006). Intracellular localization of ClC chloride channels and their ability to form hetero-oligomers. *J Cell Physiol* **206**, 792–798.

Tzfira T, Tian GW, Lacroix B, Vyas S, Li J, Leitner-Dagan Y, Krichevsky A, Taylor T, Vainstein A & Citovsky V (2005). pSAT vectors: a modular series of plasmids for autofluorescent protein tagging and expression of multiple genes in plants. *Plant Mol Biol* **57**, 503–516.

Yoo SD, Cho YH & Sheen J (2007). Arabidopsis mesophyll protoplasts: a versatile cell system for transient gene expression analysis. *Nat Protoc* **2**, 1565–1572.

Author contributions

F.G. and A.Ca. had the idea, A.Co., P.V.K.G., A.B., M.P. and F.L.S. contributed to the design of the experiments. A.Co., M.F. and B.B. designed vectors, performed protoplast transformation and analysed confocal images (at the University of Padova). At IBF-CNR Genova, P.V.K.G., A.B. and A.Ca. performed protoplast transformation, patch-clamp recordings on isolated vacuoles and analysed and interpreted data, with contributions of J.S.-S. I.Z. and M.P. performed two-electrode voltage-clamp on *Xenopus* oocytes and analysed data (IBF-CNR Genova). J.S.-S. and A.Ca. wrote the paper with the help of A.B. A.Co., P.V.K.G., B.B., M.P., F.L.S. and F.G. revised the paper. A.Ca. coordinated the project. All authors approved the final version of the manuscript.

Acknowledgements

We thank Rainer Hedrich (University of Würzburg, Germany), Anna Moroni (University of Milan, Italy), Shin Hamamoto (Tohoku University, Japan) and Cristiana Picco (IBF-CNR, Italy) for critical reading of the manuscript and Sandro Vitale (IBBA-CNR, Italy) for interesting discussions. We thank Giovanna Loro (University of Padova, Italy) for support with molecular biology. Original clones were kindly provided by T. J. Jentsch (Leibniz-Institut für Molekulare Pharmakologie/Max-Delbrück-Centrum für Molekulare Medizin, Berlin, Germany). Supported by Telethon Italy (grant GGP08064), the EU Research Training Network 'VaTEP', Progetti di Ricerca di Interesse Nazionale (bando 2008, to A.Ca.), the Compagnia San Paolo and the Italian Institute of Technology (SEED project). This paper is dedicated to the memory of our colleague and friend Paolo Giacinto Pezzuto.

Authors' present addresses

A. Costa: Università degli Studi di Milano, Dipartimento di Biologia, Via G. Celoria 26, 20133 Milano, Italy.

P. V. K. Gutla: Laboratory of Plant Physiology and Biophysics, Institute of Molecular Cell and Systems Biology, University of Glasgow, UK.